Advanced Composite High-κ Gate Stack for Mixed Anion Arsenide-Antimonide Quantum Well Transistors

A. Ali, H. Madan, R. Misra, E. Hwang, A. Agrawal, I. Ramirez, P. Schiffer, T. N. Jackson, S. E. Mohney, J. B. Boos[1], B. R. Bennett[1], I. Geppert[2], M. Eizenberg[2] and S. Datta
Penn State University, University Park, PA, USA;
[1]Naval Research Lab, Washington, DC, USA; [2]Technion - Israel Institute of Technology University, Haifa, Israel;
Tel: (814) 865-0519, Fax: (814) 865-7065, Email: aua176@psu.edu

Abstract

This paper demonstrates the integration of a composite high-κ gate stack (3.3 nm Al_2O_3-1.0 nm GaSb) with a mixed anion $InAs_{0.8}Sb_{0.2}$ quantum-well field effect transistor (QWFET). The composite gate stack achieves; (i) EOT of 4.2 nm with <10^{-7}A/cm^2 gate leakage (ii) low D_{it} interface (~1x10^{12} /cm^2/eV) (iii) high drift μ of 3,900-5,060 cm^2/V-s at N_S of 5x10^{11}-3x10^{12}/cm^2. The $InAs_{0.8}Sb_{0.2}$ MOS-QWFETs with composite gate stack exhibit extrinsic (intrinsic) g_m of 334 (502) μS/μm and drive current of 380 μA/μm at V_{DS} = 0.5V for Lg=1μm.

Introduction

Mixed anion $InAs_ySb_{1-y}$ quantum-wells (QW) with high electron mobility are candidates for integration with high hole mobility $In_xGa_{1-x}Sb$ QW for ultra-low power complementary applications[1]. With the exception of a recent $In_{0.7}Ga_{0.3}As$ QWFET with high-κ gate stack[2], nearly all QWFETs, reported to date, use Schottky gates and suffer from high gate leakage. For further scaling, a gate stack is needed for integration with $InAs_ySb_{1-y}$ QWFET, with low EOT and J_{OX}, good interface properties and high carrier mobility in the channel. Here, we integrate a composite high-κ gate stack (Al_2O_3-GaSb) with $InAs_{0.8}Sb_{0.2}$ QWFET, resulting in high performance transistors operating at 0.5V V_{DS}.

Materials Characterization

MBE grown mixed anion $InAs_ySb_{1-y}$ QW exhibit room temperature electron mobility between 11,000-22,000 cm^2/V-s with varying electron density[3], corresponding to ballistic mean free path of ~400nm, making them promising channel material candidates for high-speed, low power electronics (**Fig. 1**). To retain the high carrier mobility in $InAs_{0.8}Sb_{0.2}$ QWFET, the high-κ dielectric is deposited on the upper barrier and not directly on the channel. We incorporated an ultra-thin (1nm) GaSb layer in the upper barrier as it avoids Al at the interface and associated surface oxidation. Using n-type and p-type GaSb(100) MOS capacitors, we evaluated both ALD and Plasma Enhanced ALD (PEALD) Al_2O_3 dielectrics and confirmed unpinned Fermi level in GaSb MOS system with the latter (**Fig. 2a**)[4]. By minimizing elemental Sb at the GaSb/Al_2O_3 interface using the low temperature PEALD Al_2O_3, we demonstrate low D_{it} (~1x10^{12} /cm^2/eV) near the valence band making the composite 3.3nm Al_2O_3/1nm GaSb gate stack suitable for $InAs_{0.8}Sb_{0.2}$ QWFETs, where the surface Fermi level sweeps below the midgap of GaSb towards the valence band (**Fig. 2b**). From XPS measurements we estimate the valence and conduction band offsets to be 3.4eV and 2.4eV respectively, sufficient for gate leakage suppression (**Figs. 4a,b**). **Fig. 3** shows the schematic of the $InAs_{0.8}Sb_{0.2}$ MOS QWFET with GaSb and Al_2O_3 dielectric which forms a composite gate stack on top of the QW. **Fig. 5** shows the energy band diagram of the $InAs_{0.8}Sb_{0.2}$ QW structure with the composite Al_2O_3-GaSb gate stack using Schrodinger-Poisson simulation, indicating strong electron confinement in the $InAs_{0.8}Sb_{0.2}$ QW. **Figs. 6a,b** show the TEM micrographs of the $InAs_{0.8}Sb_{0.2}$ QWFET stack grown on GaAs by MBE and the active device layers. Hall measurements were performed on the device layers by varying the temperature from 4K-300K (**Figs. 7a,b**). **Table 1** shows the percentage contribution to 1/μ from individual scattering mechanisms at 300K. Near the room temperature, intra and inter sub-band acoustic deformation potential (ADP) scattering and interface defect scattering[5] dominate. Shubnikov-de Haas (SdH) oscillations (**Fig. 8a**) are observed at low temperature (2-15K) and high magnetic fields (0-9Tesla) confirming excellent channel and interface quality. An effective mass of 0.043m_0 is extracted from the temperature dependence of the amplitude of SdH oscillations, which is lower than 0.05m_0 reported for InAs QW due to quantization and band non-parabolicity[6]. FFT of SdH oscillations vs. 1/B at 2K (**Fig. 8b**) shows single peak confirming majority carrier transport in the first subband of the QW at n_s=2x10^{12}/cm^2 and no parallel conduction.

Device Characterization

Figs. 9a,b show the top view SEM and cross-section TEM of the $InAs_{0.8}Sb_{0.2}$ MOS QWFET with 100nm physical gate length (L_G) and the composite Al_2O_3-GaSb gate stack. Pd/Pt/Au metal stack was alloyed to form embedded contacts making direct contact with the QW (**Fig.10**). Circular TLM measurements before and after PEALD Al_2O_3 deposition are shown in **Fig. 11**. **Figs. 12a,b** show the split C-V_G characteristics of $InAs_{0.8}Sb_{0.2}$ MOS-QWFET for 4.4nm and 3.3nm physically thick Al_2O_3 and the frequency dispersion characteristics. The EOT of the thinner stack is 4.2 nm which includes the 9 nm $Al_{0.8}In_{0.2}Sb$ barrier and 12 nm $InAs_{0.8}Sb_{0.2}$ QW capacitance. Conductance vs frequency contour plot (**Figs. 13a,b**) shows positive slope with V_G indicating electron capture/emission process. This could be due to

the traps at the oxide-GaSb interface. **Fig. 14** plots J_{OX} vs V_G showing less than 10^{-7} A/cm^2 of gate leakage in $InAs_{0.8}Sb_{0.2}$ MOS-QWFET. Room temperature drift mobility values of 3,900-5,060 cm^2/V-s at carrier concentrations of $5x10^{11}$-$3x10^{12}$/cm^2 are extracted from split C-V_G data (**Fig. 15**). **Figs. 16-17** show the drain current (I_D) vs. gate voltage (V_G) of $InAs_{0.8}Sb_{0.2}$ MOS-QWFET for various L_G and L_{SIDE}. Parasitic access resistance limits the achievable on-current in the fabricated devices. For the shortest L_{SIDE} of 0.25µm and L_G = 1µm, the best extrinsic g_m and I_D at 300K are 334 µS/µm and 380 µA/µm, and at 77K are 630 µS/µm and 411 µA/µm at V_{DS} = 0.5V. Peak intrinsic gm increases to 502 µS/µm (1,070µS/µm) at 300K (77K) (**Fig. 19**). **Fig. 18** shows the output characteristics of the device at 300K and 77K for L_G = 1µm and L_{SIDE} = 0.25 µm. The high off-state leakage of $InAs_{0.8}Sb_{0.2}$ MOS-QWFET at 300K is likely due to the hole accumulation in the $Al_{0.8}In_{0.2}Sb$ barrier layer screening the gate potential as well as the generation of holes due to impact ionization. The source side effective injection velocity, V_{eff}, is extracted as a function of V_{GSi} - V_T at 77K for $InAs_{0.8}Sb_{0.2}$ MOS-QWFET (**Fig. 20**). The highest V_{eff} obtained is $1.4x10^7$ cm/s, one of the highest values ever reported for III-V MOS QWFETs.

Conclusions

An advanced composite high-κ gate stack (3.3nm Al_2O_3-1.0nm GaSb) is successfully integrated in the mixed anion $InAs_{0.8}Sb_{0.2}$ QWFET with low EOT (4.2nm), negligible J_{OX} (10^{-7} A/cm^2) and high drift µ (3,900-5,060 cm^2/V-s). The $InAs_{0.8}Sb_{0.2}$ MOS-QWFETs with Lg = 1 µm exhibit intrinsic transconductance of 502 µS/µm and 1,070 µS/µm and drive currents of 380 µA/µm and 411 µA/µm at room temperature and 77K, respectively, all at V_{DS} = 0.5V.

References

[1]J. B. Boos et al., *IEICE Trans*. vol. E85-A/B/C/D, no. 7, July (2008) [2]M. Radosavljevic et al., *IEDM Tech. Dig*. pp. 319, Dec (2009) [3]B. P. Tinkham, et al., *J. Vac. Sci. Technol.* B 23, pp. 1441 (2005) [4]A. Ali et al., *Dev. Res. Conf.* June (2010) [5]C. Nguyen et al., Appl. Phys. Lett. pp. 1854 (1992) [6]D. Jin et al., *IEDM Tech Dig*., pp. 495 (2009)

Acknowledgement

We acknowledge financial support from DARPA/SRC sponsored MARCO-MSD Center.

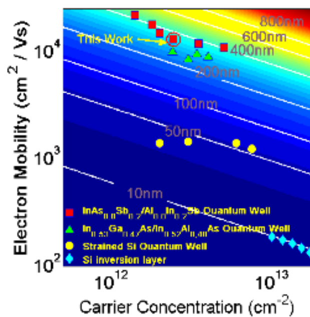

Fig. 1 Electron mobility vs carrier concentration overlayed on a contour map of ballistic mean free path

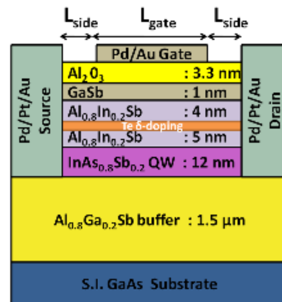

Fig. 3 Schematic of $InAs_{0.8}Sb_{0.2}$ MOS QWFET on GaAs substrate with 1nm GaSb and 3.3nm PEALD Al_2O_3 dielectric which forms a composite Al_2O_3-GaSb gate stack on top of QW

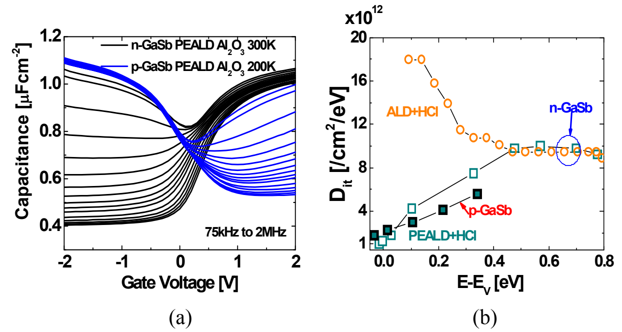

Fig. 2 (a) Unpinned C-V characteristics of n-type and p-type GaSb (100) MOS capacitors with PEALD Al_2O_3 (b) D_{it} of 1-3 x 10^{12}/cm^2/eV near E_V achieved with PEALD Al_2O_3 samples

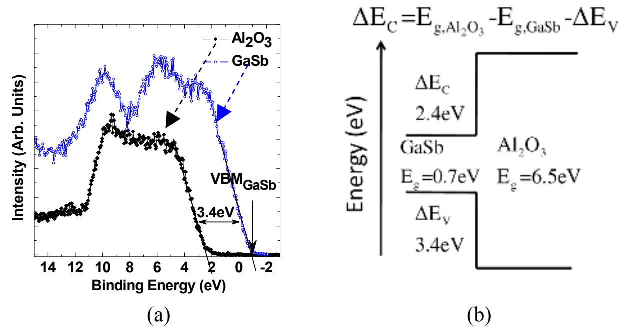

Fig. 4 (a) Measured energy difference between the valence band spectra of Al_2O_3 and GaSb (100) gives valence band offset of 3.4eV (b) Valence and conduction band offsets derived from XPS analysis

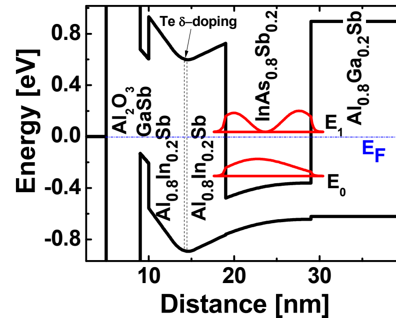

Fig. 5 Band diagram of $InAs_{0.8}Sb_{0.2}$ MOS QWFET with 1nm GaSb and 3.3nm PEALD Al_2O_3 dielectric from Schrodinger-Poisson simulation

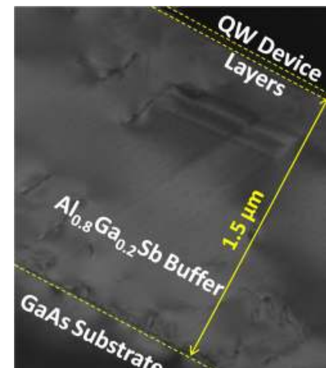

Fig. 6 (a) Cross-sectional TEM micrograph of $InAs_{0.8}Sb_{0.2}$ QW stack on GaAs substrate using $Al_{0.8}Ga_{0.2}Sb$ relaxed buffer layer

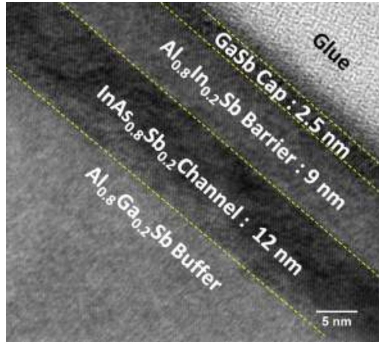

Fig. 6 (b) High resolution TEM micrograph of $InAs_{0.8}Sb_{0.2}$ QW stack with as deposited 2.5nm GaSb (surface preparation prior to oxide deposition reduces GaSb thickness to 1nm)

	% contribution to 1/µ at 300K
Interface Charge	50%
ADP Scattering	23%
Remote Ionized Impurity Scattering	13%
Alloy Scattering	8%
Polar Optical Phonon Scattering	6%

Table 1 Percentage contribution to $1/\mu_{Total}$ at 300K

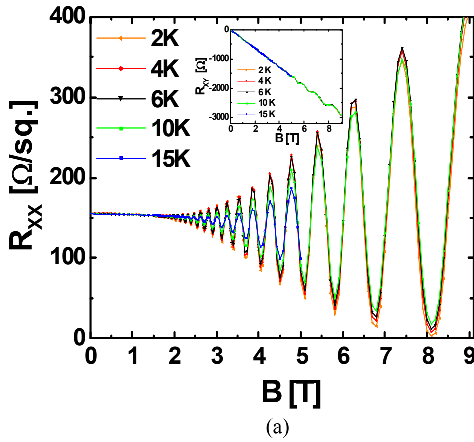

(a)

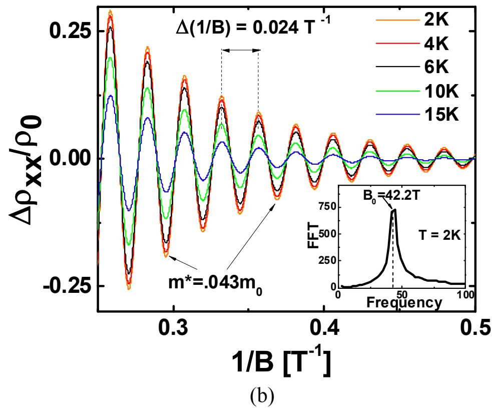

(b)

Fig. 8 (a) Shubnikov-de Haas (SdH) oscillations in the sheet resistance. Temperature dependence of the amplitude of these oscillations is used to calculate **m*** (b) FFT of SdH oscillations vs. 1/B at 2K (inset) shows single peak confirming majority carrier transport in the first subband of the QW at n_s=2x10^{12}/cm^2 and no parallel conduction

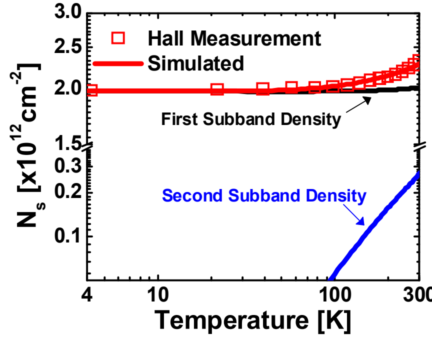

(a)

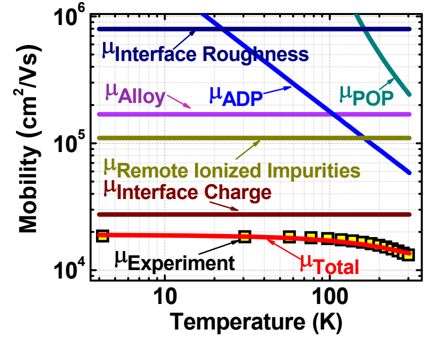

(b)

Fig. 7 (a) Carrier density (N_s), and (b) Hall mobility vs temperature for $InAs_{0.8}Sb_{0.2}$ QW

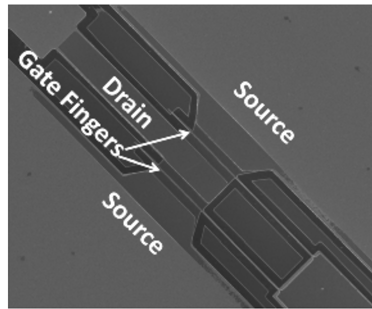

Fig. 9 (a) Top view SEM of $InAs_{0.8}Sb_{0.2}$ QWFET with composite Al_2O_3-GaSb gate stack on top of the QW

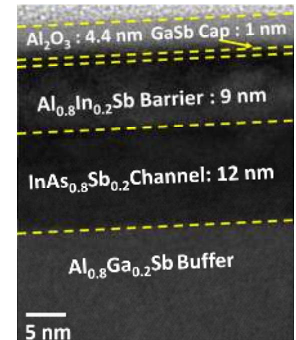

Fig. 9 (b) Cross-section TEM of $InAs_{0.8}Sb_{0.2}$ MOS QWFET with 1.0nm GaSb-4.4nm PEALD Al_2O_3 composite gate stack on top of the QW

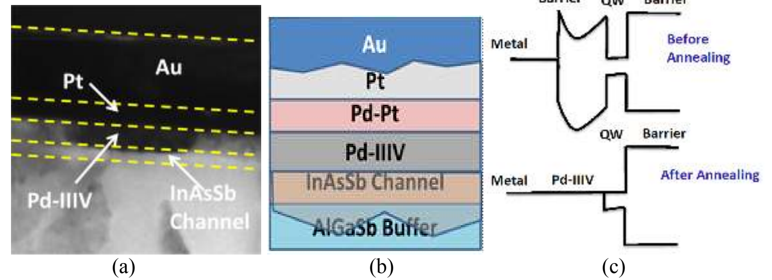

(a) (b) (c)

Fig. 10 (a) Cross-section TEM of $InAs_{0.8}Sb_{0.2}$ MOS QWFET under the alloyed embedded contact directly contacting the $InAs_{0.8}Sb_{0.2}$ channel (b) Schematic cross-section of the region underneath the ohmic contact (c) Band diagram explaining the embedded ohmic contact formation

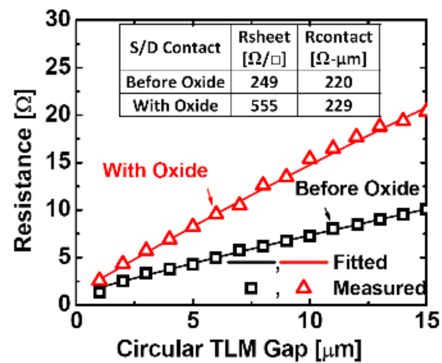

Fig. 11 Circular TLM measurements before and after PEALD Al_2O_3 deposition

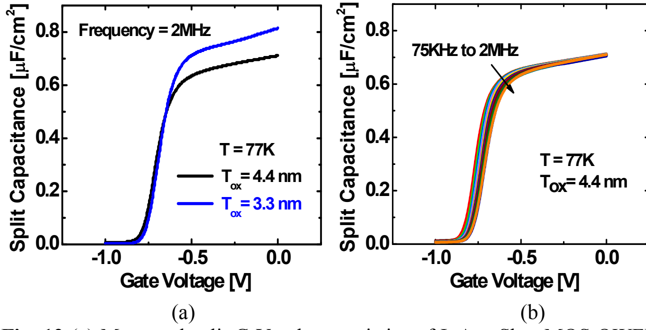

Fig. 12 (a) Measured split C-V_G characteristics of $InAs_{0.8}Sb_{0.2}$ MOS QWFET with various composite gate stack thickness (b) Frequency dispersion of the C-V_G characteristics of $InAs_{0.8}Sb_{0.2}$ MOS QWFET

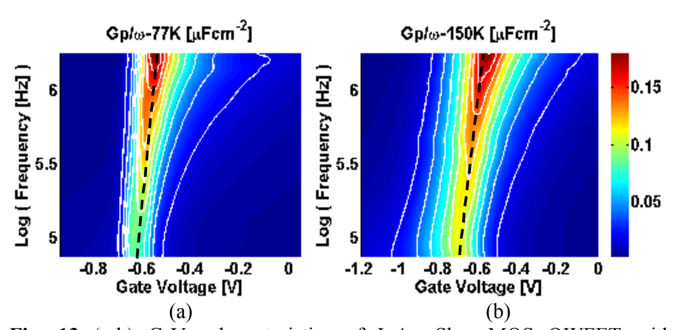

Fig. 13 (a-b) G-V_G characteristics of $InAs_{0.8}Sb_{0.2}$ MOS QWFET with composite gate stack; peak conductance trace reflects Fermi level movement in the $InAs_{0.8}Sb_{0.2}$ QW

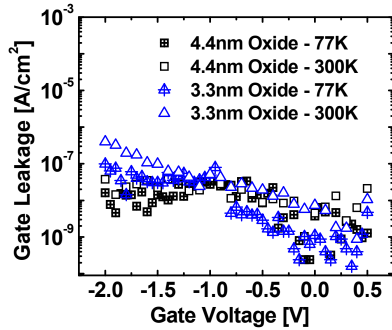

Fig. 14 J_{OX} vs V_G showing lower than 10^{-7} A/cm^2 of gate leakage in $InAs_{0.8}Sb_{0.2}$ MOS-QWFET

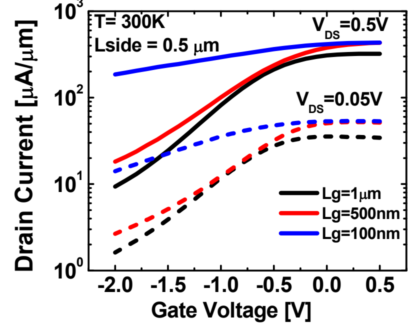

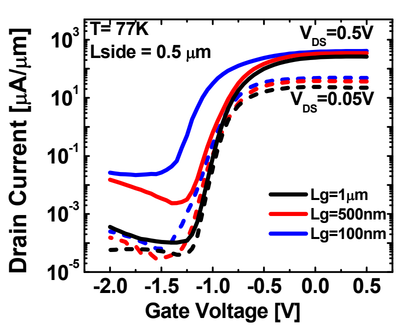

Fig. 16 L_G scaling: Drain current (I_D) vs. gate voltage (V_G) of $InAs_{0.8}Sb_{0.2}$ MOS-QWFET with L_G= 1 μm, 500nm, 100nm and Al_2O_3-GaSb composite stack (EOT= 4.2nm) at 300K and 77K at V_{DS} = 0.5V, 50mV (L_{SIDE} = 0.5 μm)

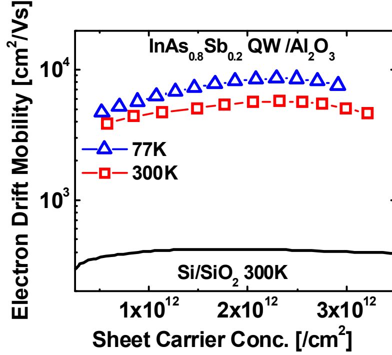

Fig. 15 Drift μ vs N_s at 77K and 300K in $InAs_{0.8}Sb_{0.2}$ MOS QWFET from split C-V_G measurements

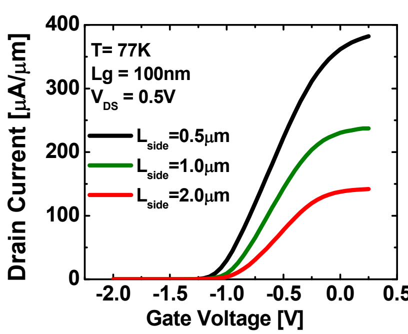

Fig. 17 L_{SIDE} scaling: I_D vs. V_G of L_G= 100nm $InAs_{0.8}Sb_{0.2}$ MOS-QWFET with composite stack at 77K at V_{DS} = 0.5Vwith L_{SIDE} = 0.5, 1 and 2 μm

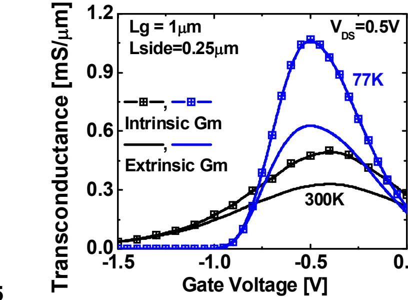

Fig. 19 Transconductance (g_m) characteristics of $InAs_{0.8}Sb_{0.2}$ MOS-QWFET with L_G= 1 μm, L_{SIDE} = 0.25 μm and Al_2O_3-GaSb composite stack (EOT= 4.2nm) at 300K and 77K. Intrinsic peak gm is 502 μS/ μm and 1070 μS/ μm at 300K and 77K, respectively

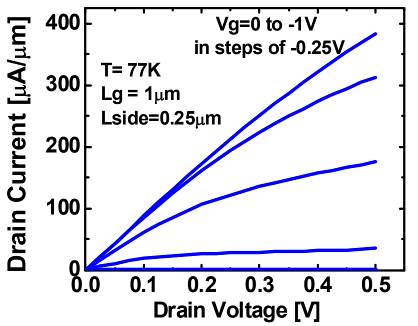

Fig. 18 Output Charactersitics: I_D vs. V_{DS} of $InAs_{0.8}Sb_{0.2}$ MOS-QWFET with L_G= 1 μm, L_{SIDE} = 0.25 μm and Al_2O_3-GaSb composite stack (EOT= 4.2nm) at 300K and 77K

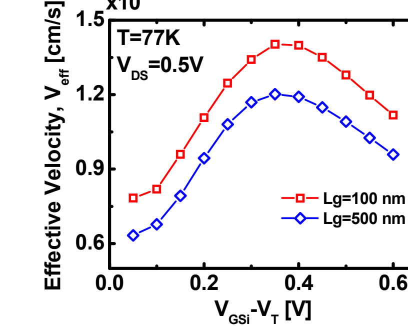

Fig. 20 Extracted effective injection velocity, V_{eff}, as a function of V_{GSi}-V_T using the charge obtained from split C-V_G measurements and $I_{D,SAT}$ vs V_{GSi}-V_T. The V_T from split C-V_G is matched to the $V_{T,SAT}$ from $I_{D,SAT}$ vs V_{GSi}-V_T to obtain V_{eff}